



Is the Caudate, Putamen, and Globus Pallidus the Delusional Disorder's Trio? A Texture Analysis Study

Murat Baykara¹ 
Sema Baykara^{2,*} 

¹Department of Radiology, Haydarpasa Numune Training and Research Hospital, 34668 Istanbul, Türkiye
²Department of Psychiatry, Erenkoy Psychiatry and Neurology Training and Research Hospital, 34736 Istanbul, Türkiye

Abstract

Background: The neurobiological basis of delusional disorder is less explored through neuroimaging techniques than in other psychotic disorders. This study aims to provide information about the neural origins of delusional disorder (DD) by examining the neuroanatomical features of some basal nuclei with magnetic resonance imaging (MRI) texture analysis.

Materials and Methods: Twenty DD patients and 20 healthy individuals were included in the study. Globus pallidus, putamen, and caudate nuclei were selected individually with a region of interest (ROI) on the axial MRI images. The entire texture analysis algorithm applied to all selected ROIs was done with an in-house software. Nuclei on both sides were taken as separate samples.

Results: There were no significant differences between groups in terms of age and gender. The average “mean, median and maximum” values of all three nuclei were decreased in DD patients. The small putamen area and the differences detected in different tissue parameters for all three nuclei in delusional disorder patients indicate that they differ in delusional disorder from normal controls ($p < 0.05$).

Conclusion: The differences detected in the texture parameters for all three nuclei indicate that there is something different in the DD from in the normal controls. Neuroimaging studies with larger samples and different techniques in the future may shed light on the etiology of delusional disorder.

*Corresponding author details: Sema Baykara, Department of Psychiatry, Erenkoy Psychiatry and Neurology Training and Research Hospital, 34736 Istanbul, Türkiye. Email: semabaykara@hotmail.com

Keywords

delusional disorder; caudate nucleus; putamen; globus pallidus; computer-assisted image processing; magnetic resonance imaging

Introduction

Delusional disorder (DD) is a relatively rare mental disorder characterized by the presence of one or more delusions that have been present for at least 1 month. Apart from the behavioral consequences associated with delusions, patients do not appear strange and impairments in psychosocial functioning may be more limited than those seen in other psychotic disorders [1,2]. According to the Diagnostic and Statistical Manual of Mental Disorders, Fifth Edition (DSM-5) criteria, delusional disorder is distinguished from schizophrenia by the absence of prominent auditory or visual hallucinations and the absence of impairment in functional areas outside the delusional scope [3]. Patients develop fixed abnormal beliefs that are often persecuting in nature, although they may take other forms [1]. Delusional disorder has a later onset age than schizophrenia and does not show gender dominance [4,5]. The cause of delusional disorder is unknown, but genetic, biochemical, and environmental factors are thought to play an important role in its development [6–11]. In terms of etiopathogenesis and clinical features, delusional disorder has not been well studied compared to schizophrenia and other psychotic disorders. Much of the information in the chapters on etiology, course and treatment is based on small samples or clinical observations. To date, very few studies in a small number of patients have examined genetic predisposition [12,13] and structural brain changes [14,15] in DD, but the findings of these studies were mainly inconclusive.

Patients with bilateral basal ganglia calcification, defined as Fahr's syndrome (familial idiopathic basal ganglia

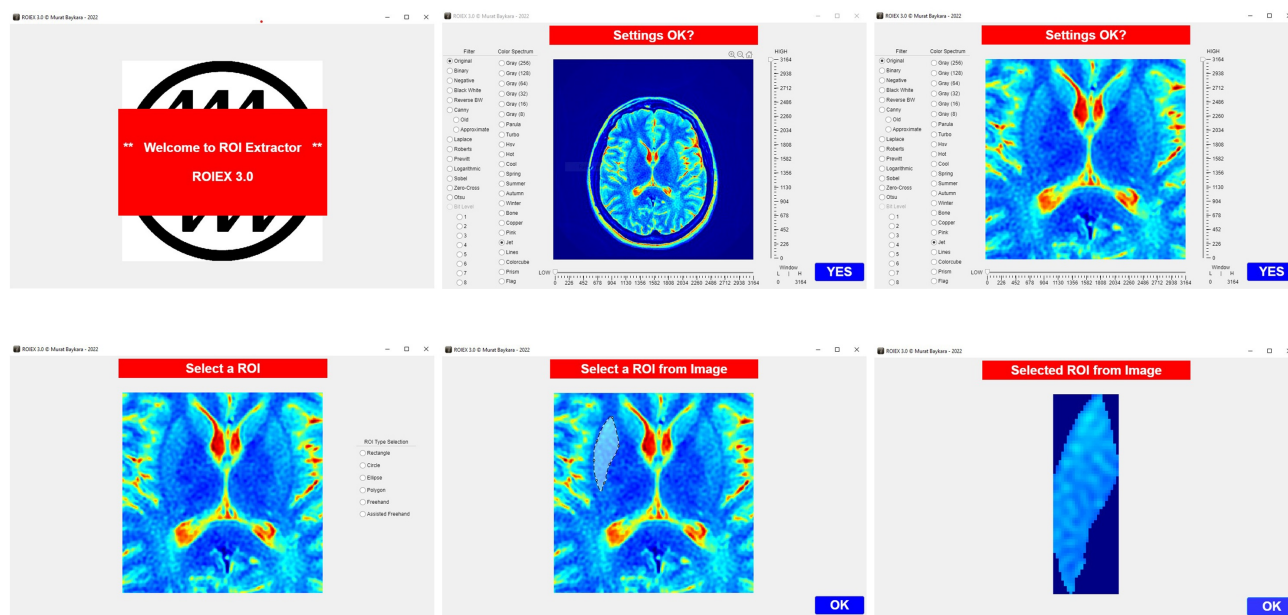


Fig. 1. Demonstration of region of interest (ROI) removal of the right putamen nucleus.

calcification) have been described in the literature [16–19]. Psychiatric features such as cognitive symptoms, psychotic symptoms accompanied by delusions, and mood disorders were observed in 40% of these patients [19]. The computed tomography (CT) scans of these patients showed calcified hyperintensities in the basal ganglia (usually restricted to the globus pallidus) but caudate nucleus, thalamus, dentate nucleus, the putamen, and white matter may also be affected [20,21]. A review study examining the etiopathogenesis of schizophrenia also stated that the basal ganglia may play a role in the development of psychosis [22]. This information in the literature suggests that the basal ganglia may play a role in the etiology of delusional disorder, which is a psychotic disorder accompanied by delusions.

Texture analysis is basically a technique that evaluates the spatial position and intensity of signal features in imaging, i.e., unique pixels in digital images. Texture properties are essentially mathematical parameters calculated from the pixel distribution obtained with the tissue type and therefore characterize the basic structure of the objects shown in the image. By quantitatively assessing the spatial variation and distribution of grayscale levels in the region of interest (ROI), it provides a more objective and detailed assessment of tissue characteristics than visual analysis by human observers [23–26]. Entropy measures parametric homogeneity in the ROI. It is a parameter that indicates irregularity in the intensity. The value increases as the distribution becomes irregular [27]. Skewness shows the asymmetry of the distribution; if there are more points on the left side of

the mean, the skewness is positive. Kurtosis is a measure of the peak of distribution. If the histogram is bell curve, kurtosis is three, and if the histogram has a sharper peak, it is greater than three [28].

It is the literature that seen in texture-based studies have not yet been conducted in delusional disorder patients. In this study, it was aimed to examine the basal ganglia (because they can be accessed and evaluated with accuracy in magnetic resonance imaging (MRI) images) of patients diagnosed with delusional disorder with MRI based texture analysis and to investigate possible differences from normal ones.

Materials and Methods

Study Population

The inclusion criteria of the study were: Between 18 and 65 years of age, to have no other psychiatric diagnosis, no intellectual, no neurological or physiological disease. To have no history of alcohol or substance use in the last 6 months. To have no contraindications for MRI examinations.

The exclusion criteria were: To be under 18 years and above 65 years. To have any psychiatric or physiological diagnoses. To have any alcohol or substance use history in the last 6 months. To be illiterate.

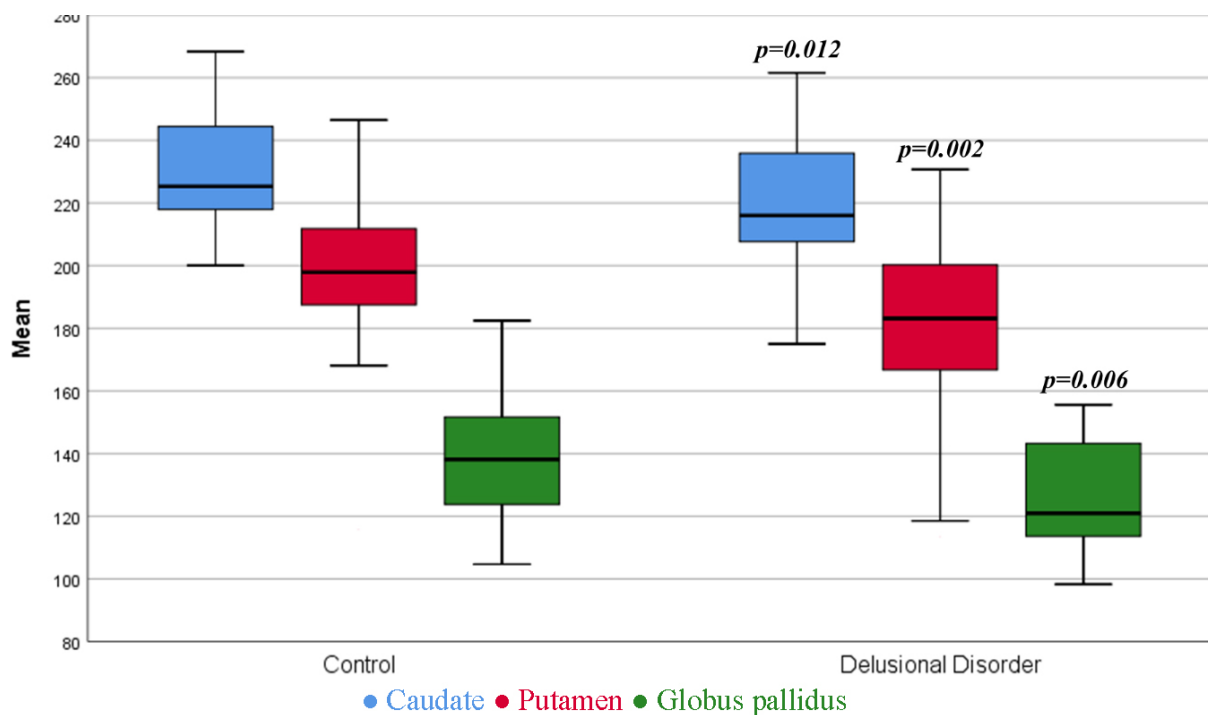


Fig. 2. The change of the “mean” value according to the nuclei is shown with a box-plot chart. NOTE: Mean, p -value for intergroup comparisons, see Tables 1,2,3. Error bar for maximum and minimum values. Mann-Whitney U Test was used for intergroup comparisons.

Twenty patients who met all criteria and were diagnosed with delusional disorder according to the DSM-5 [3] criteria were studied. These criteria were applied using the hospital information system. The diagnosis of the patients was confirmed after a psychiatric evaluation by a psychiatrist with 15 years of experience. Participants were respectively selected from the hospital information system. As the control group, 20 age and gender equivalent healthy individuals who met the study criteria and did not have a psychiatric diagnosis were selected. Since the study was retrospective and based on old records, no informed consent was obtained.

Analysis of Images

A 1.5 T Philips Ingenia scanner (Philips Medical System, Best, NL) with an 8-channel array head coil was used for MRI. High resolution sagittal 3D-T2-FLAIR Turbo Spin Echo MRI images were obtained.

Images were transferred from the Picture Archiving Communication Systems (PACS) to a separate storage medium in DICOM (Digital Imaging and Communications in Medicine) image format. Then the images were transferred to a Windows 10 (Microsoft Corporation, Seattle, WA, USA) based computer and processed to obtain the final data. The entire analysis algorithm applied to all selected

images was done with an in-house software coded in MATLAB (version R2021b; MathWorks, Natick, MA, USA).

All regions of the globus pallidus, putamen, and caudate nuclei were selected individually in the axial reformat images that best represent the anatomy, without exceeding their borders, with an ROI determined by a senior radiologist (M.B.) [29,30] (Fig. 1). The nuclei of both sides were taken as separate samples.

Histogram and fractal analysis texture analysis values obtained from ROIs have been previously described in the literature [23,25,26,30,31].

Statistical Analysis

Data are presented as mean \pm standard deviation and 1st, 2nd and 3rd percentiles. The statistical analyses were conducted with IBM SPSS for Windows, version 25.0 (IBM statistics for Windows version 25, IBM Corporation, Armonk, NY, USA). The normality of the distribution of the data was analyzed with the Kolmogorov–Smirnov test. Based on the test findings, Mann-Whitney U test was used to compare the groups due to abnormal distribution of data. The chi-square test was used for the count data. $p < 0.05$ was accepted as statistically significant.

Table 1. Texture analysis parameters investigated for caudate nucleus. The nuclei on both sides were used as separate samples.

Caudate	Control (40)					Delusional disorder (40)					Z	p
	Mean	Std. Deviation	Percentiles			Mean	Std. Deviation	Percentiles				
			25	50	75			25	50	75		
Pixel Count of ROI	188.73	41.54	162.00	192.00	217.50	189.15	45.82	147.50	191.00	218.00	-0.149	0.881
Mean	230.81	18.00	217.90	225.28	244.47	219.34	18.84	207.27	215.99	236.34	-2.521	0.012
Standard Deviation	18.28	3.64	16.54	18.21	19.95	17.57	3.60	14.86	17.31	20.62	-0.885	0.376
Median	231.94	18.20	219.13	228.00	246.25	219.53	19.26	207.00	215.50	236.88	-2.575	0.010
Mean Absolute Deviation	14.20	2.88	12.87	14.03	15.92	13.75	2.78	11.62	13.77	16.13	-0.462	0.644
Median Absolute Deviation	11.16	2.48	10.00	11.00	12.00	11.23	2.51	9.13	11.00	13.00	-0.213	0.831
Minimum	175.75	23.02	161.25	171.50	193.75	170.05	20.62	155.25	170.00	185.75	-0.914	0.361
Maximum	278.63	24.95	262.25	274.00	293.50	266.95	23.77	254.00	265.00	278.50	-2.276	0.023
Variance	347.00	142.45	273.62	331.59	397.89	321.20	129.56	220.99	299.70	425.02	-0.885	0.376
Range	102.88	22.07	89.50	103.50	120.75	96.90	24.65	75.75	98.00	109.00	-1.376	0.169
Interquartile Range	22.79	4.99	20.06	22.13	25.75	22.71	4.96	18.81	23.13	26.38	-0.116	0.908
Most Frequent Value	233.80	19.09	220.25	232.00	247.25	218.80	20.60	207.25	216.50	233.00	-2.974	0.003
Size %L	14.73	2.21	13.10	15.00	16.03	15.55	1.98	14.66	15.68	17.08	-1.737	0.082
Size %M	71.01	2.95	69.03	71.47	73.28	69.23	3.58	66.94	68.98	70.96	-2.497	0.013
Size %U	14.25	1.72	12.98	14.50	15.50	15.22	2.36	13.56	15.26	16.35	-2.088	0.037
Kurtosis	3.65	0.76	3.10	3.52	4.16	3.44	1.34	2.65	3.18	3.56	-2.242	0.025
Skewness	-0.2652	0.5599	-0.6937	-0.3135	0.1833	-0.0795	0.5358	-0.3356	-0.0072	0.2470	-1.867	0.062
Smoothness	0.0034	0.0015	0.0025	0.0030	0.0036	0.0037	0.0016	0.0023	0.0033	0.0045	-0.885	0.376
Root-Mean-Square Level	231.55	17.98	218.95	226.15	245.33	220.06	18.85	208.32	216.44	236.75	-2.502	0.012
Root-Sum-of-Squares Level	3165.69	491.10	2815.98	3133.27	3496.49	2999.19	401.68	2706.61	3040.77	3263.25	-1.386	0.166
1st Percentile	183.11	21.90	167.11	178.23	202.95	177.54	18.59	164.58	177.02	191.40	-0.953	0.341
3rd Percentile	192.34	20.06	181.43	186.62	208.46	185.60	18.32	173.48	186.82	197.76	-1.054	0.292
5th Percentile	198.52	19.49	186.08	192.23	214.73	189.83	18.32	177.00	191.50	202.21	-1.535	0.125
10th Percentile	207.34	18.43	194.08	201.10	219.23	196.45	18.54	184.20	197.70	208.88	-2.136	0.033
25th Percentile	219.96	17.86	205.06	215.38	233.00	208.12	18.87	194.81	207.13	224.50	-2.469	0.014
75th Percentile	242.74	18.46	232.00	238.25	258.88	230.83	19.87	217.63	227.75	247.50	-2.363	0.018
90th Percentile	252.89	19.14	242.33	249.70	267.93	241.11	19.65	229.20	238.35	254.83	-2.420	0.016
95th Percentile	258.36	19.50	246.48	255.50	271.65	247.54	20.11	233.33	245.75	259.31	-2.367	0.018
97th Percentile	262.83	20.39	250.25	260.74	275.89	251.94	21.65	238.04	250.83	261.04	-2.497	0.013
99th Percentile	271.39	21.46	256.06	270.06	285.03	259.97	22.64	244.47	258.05	271.98	-2.454	0.014

Table 1. Continued.

Caudate	Control (40)					Delusional disorder (40)					Z	p
	Mean	Std. Deviation	Percentiles			Mean	Std. Deviation	Percentiles				
			25	50	75			25	50	75		
<i>Entropy</i>	3.82	0.40	3.47	3.83	4.10	4.05	0.42	3.83	4.13	4.26	-2.752	0.006
Uniformity	0.3071	0.0703	0.2657	0.3013	0.3456	0.3166	0.0558	0.2691	0.3108	0.3548	-0.962	0.336
<i>Mean Local Entropy</i>	3.00	0.35	2.71	2.99	3.24	3.22	0.36	2.98	3.27	3.45	-2.887	0.004
Mean Local Range	89.68	10.77	81.36	89.37	95.25	91.00	12.28	82.00	90.64	99.62	-0.491	0.624
Mean Local Standard Deviation	36.35	4.66	32.68	36.03	38.77	36.75	5.01	33.30	36.62	40.49	-0.443	0.658
Contrast	56.12	24.66	43.78	57.63	71.54	53.67	19.86	40.94	51.94	65.50	-1.001	0.317
Correlation	0.0383	0.3145	-0.0715	-0.0010	0.0441	-0.0091	0.2668	-0.0937	-0.0412	0.0195	-1.511	0.131
Energy	0.0057	0.0017	0.0046	0.0052	0.0062	0.0056	0.0014	0.0046	0.0053	0.0068	-0.154	0.878
Homogeneity	0.2413	0.0560	0.2110	0.2200	0.2619	0.2442	0.0363	0.2196	0.2332	0.2597	-1.184	0.237
<i>Higuchi Fractal Dimension</i>	1.20	0.07	1.15	1.19	1.23	1.25	0.08	1.18	1.24	1.31	-2.829	0.005
<i>Katz Fractal Dimension</i>	1.31	0.14	1.31	1.32	1.34	1.38	0.12	1.32	1.34	1.41	-2.637	0.008
Hausssdorf Fractal Dimension	1.49	0.08	1.44	1.49	1.52	1.51	0.08	1.45	1.49	1.55	-0.770	0.441
Box-Counting Fractal Dimension	1.53	0.08	1.47	1.52	1.57	1.53	0.09	1.47	1.53	1.57	-0.029	0.977

Mann-Whitney U Test. NOTE: Indicators with $p < 0.05$ are bolded and italicized.

Table 2. Texture analysis parameters investigated for putamen nucleus. The nuclei on both sides were used as separate samples.

Putamen	Control (40)					Delusional disorder (40)					Z	p
	Mean	Std. Deviation	Percentiles			Mean	Std. Deviation	Percentiles				
			25	50	75			25	50	75		
Pixel Count of ROI	611.25	81.60	547.75	617.00	663.25	534.35	118.46	426.00	545.50	641.50	-2.858	0.004
Mean	199.68	22.40	186.31	197.86	212.42	180.93	27.72	166.10	183.13	200.42	-3.166	0.002
Standard Deviation	22.47	3.94	19.45	21.72	24.92	23.64	5.04	20.66	23.85	26.65	-1.222	0.222
Median	201.60	22.32	187.00	201.00	214.25	182.68	28.62	168.25	184.00	206.50	-3.176	0.001
Mean Absolute Deviation	18.43	3.63	15.72	17.80	20.58	19.33	4.36	16.34	19.42	22.19	-1.193	0.233
Median Absolute Deviation	16.04	3.53	13.00	15.50	18.00	16.63	4.11	14.00	17.00	19.00	-0.883	0.377
Minimum	130.80	24.36	118.00	128.00	147.75	109.43	27.78	93.75	112.00	126.50	-3.489	0.000
Maximum	256.18	23.94	245.25	256.00	270.75	239.30	32.10	218.25	244.50	263.75	-2.599	0.009
Variance	520.20	189.74	378.13	471.77	621.15	583.74	252.79	426.77	568.63	709.99	-1.222	0.222
Range	125.38	16.36	112.00	121.00	137.50	129.88	28.64	112.50	123.50	147.50	-0.722	0.470
Interquartile Range	32.91	7.77	27.00	31.63	36.75	34.25	8.69	28.44	34.50	39.00	-0.997	0.319
Most Frequent Value	206.18	24.37	190.75	207.00	223.75	185.58	33.57	173.50	190.50	207.75	-2.907	0.004
Size %L	17.44	1.99	16.40	17.41	18.30	17.50	2.36	16.52	17.58	19.25	-0.284	0.777
Size %M	66.51	3.08	65.07	66.55	68.47	66.01	3.49	62.93	66.93	68.97	-0.356	0.722
Size %U	16.05	1.68	14.88	15.76	16.96	16.49	2.05	15.03	16.54	17.96	-1.111	0.266
Kurtosis	2.74	0.44	2.44	2.69	2.99	2.78	0.60	2.38	2.55	3.01	-0.529	0.597
Skewness	-0.2355	0.2039	-0.3684	-0.2497	-0.1018	-0.2192	0.2672	-0.4204	-0.2277	0.0005	-0.366	0.715
Smoothness	0.0021	0.0007	0.0016	0.0021	0.0026	0.0021	0.0010	0.0014	0.0018	0.0023	-1.222	0.222
Root-Mean-Square Level	200.99	22.26	187.37	199.66	213.25	182.55	27.57	167.04	184.29	202.58	-3.166	0.002
Root-Sum-of-Squares Level	4969.88	728.43	4547.62	4950.28	5383.52	4209.36	837.49	3661.50	4258.01	4955.50	-3.868	0.000
1st Percentile	147.48	23.39	133.50	146.50	164.19	125.95	26.72	110.73	131.50	145.74	-3.613	0.000
3rd Percentile	156.75	24.13	142.75	154.07	175.81	135.89	26.37	120.09	142.00	152.11	-3.455	0.001
5th Percentile	161.24	23.84	149.15	159.00	181.84	141.20	26.32	124.00	148.18	158.79	-3.267	0.001
10th Percentile	169.03	23.18	156.25	166.50	187.75	148.87	26.54	133.35	155.00	167.00	-3.325	0.001
25th Percentile	183.54	22.98	169.50	181.38	200.50	164.22	27.70	151.25	167.00	185.56	-3.181	0.001
75th Percentile	216.44	22.74	204.25	217.25	228.50	198.47	28.89	181.81	199.00	221.00	-3.027	0.002
90th Percentile	227.32	23.17	216.25	228.50	239.75	210.30	29.11	192.25	212.50	234.75	-2.873	0.004
95th Percentile	233.49	22.92	222.34	233.50	247.29	216.87	29.46	197.29	219.43	242.69	-2.839	0.005
97th Percentile	237.74	22.85	227.88	237.16	253.50	220.87	29.48	201.25	223.68	245.75	-2.854	0.004
99th Percentile	245.51	22.50	237.61	247.51	260.51	229.01	29.97	209.29	233.52	253.35	-2.666	0.008

Table 2. Continued.

Putamen	Control (40)					Delusional disorder (40)					Z	p
	Mean	Std. Deviation	Percentiles			Mean	Std. Deviation	Percentiles				
			25	50	75			25	50	75		
Entropy	3.71	0.28	3.49	3.73	3.90	3.70	0.41	3.44	3.78	3.95	-0.423	0.672
Uniformity	0.2362	0.0301	0.2159	0.2329	0.2541	0.2258	0.0390	0.2026	0.2236	0.2504	-1.251	0.211
Mean Local Entropy	2.51	0.20	2.37	2.54	2.66	2.54	0.31	2.39	2.57	2.75	-0.779	0.436
Mean Local Range	50.65	4.55	47.07	50.19	54.57	50.73	8.02	44.20	49.32	56.07	-0.472	0.637
Mean Local Standard Deviation	20.45	1.93	18.99	20.26	22.11	20.20	3.25	17.52	19.71	22.45	-0.981	0.326
Contrast	319.96	104.27	242.72	286.38	396.82	275.83	111.29	190.67	253.77	332.21	-1.944	0.052
Correlation	-0.0242	0.0805	-0.0355	-0.0159	0.0023	-0.0299	0.1210	-0.0354	-0.0139	0.0193	-0.953	0.341
Energy	0.0017	0.0002	0.0015	0.0016	0.0019	0.0020	0.0005	0.0016	0.0019	0.0024	-2.983	0.003
Homogeneity	0.1345	0.0209	0.1201	0.1416	0.1483	0.1413	0.0238	0.1224	0.1413	0.1602	-0.991	0.322
Higuchi Fractal Dimension	1.22	0.04	1.19	1.23	1.25	1.24	0.04	1.21	1.24	1.26	-1.799	0.072
Katz Fractal Dimension	1.27	0.03	1.26	1.26	1.28	1.30	0.07	1.26	1.27	1.31	-2.675	0.007
Hausdorff Fractal Dimension	1.55	0.04	1.53	1.56	1.58	1.53	0.07	1.48	1.52	1.57	-2.415	0.016
Box-Counting Fractal Dimension	1.54	0.03	1.52	1.54	1.56	1.53	0.08	1.48	1.53	1.56	-1.338	0.181

Mann-Whitney U Test. NOTE: Indicators with $p < 0.05$ are bolded and italicized.

Table 3. Texture analysis parameters investigated for globus pallidus nucleus. The nuclei on both sides were used as separate samples.

Globus pallidus	Control (40)					Delusional disorder (40)					Z	p
	Mean	Std. Deviation	Percentiles			Mean	Std. Deviation	Percentiles				
			25	50	75			25	50	75		
Pixel Count of ROI	495.10	59.20	456.25	492.50	537.00	469.75	140.87	376.50	435.50	574.75	-1.626	0.104
Mean	138.86	19.38	123.67	138.14	151.85	126.78	16.94	113.47	120.97	143.62	-2.733	0.006
Standard Deviation	17.27	3.01	15.32	16.33	19.12	17.53	2.52	15.70	16.96	19.35	-0.885	0.376
Median	138.49	19.44	123.25	138.00	151.75	126.60	16.80	114.00	120.50	143.75	-2.652	0.008
Mean Absolute Deviation	13.55	2.31	11.95	12.85	15.00	13.97	2.05	12.22	13.62	15.71	-1.155	0.248
Median Absolute Deviation	11.15	2.00	10.00	11.00	12.00	11.85	2.00	10.00	11.50	13.00	-1.536	0.125
Minimum	90.18	18.86	75.50	90.50	104.75	74.63	22.49	57.25	71.00	94.25	-3.042	0.002
Maximum	196.25	26.96	176.25	193.50	207.00	179.48	22.48	159.25	176.00	196.75	-2.714	0.007
Variance	307.22	112.08	234.71	266.63	365.48	313.56	92.86	246.63	287.57	374.41	-0.885	0.376
Range	106.08	22.53	89.75	103.50	113.75	104.85	21.77	89.00	102.00	116.50	-0.385	0.700
Interquartile Range	22.34	3.99	20.00	22.00	23.94	23.81	3.98	20.63	23.00	26.75	-1.863	0.062
Most Frequent Value	137.55	20.74	123.50	134.00	150.75	126.83	16.99	113.00	122.50	143.75	-2.146	0.032
Size %L	14.92	1.33	14.42	15.26	15.80	15.82	1.52	14.89	15.57	16.99	-2.435	0.015
Size %M	69.95	2.34	68.48	69.70	71.06	68.18	2.09	66.62	68.25	69.77	-3.233	0.001
Size %U	15.13	1.43	14.51	15.02	15.84	16.00	1.37	15.15	15.73	16.85	-2.560	0.010
Kurtosis	3.40	0.90	3.03	3.16	3.65	3.05	0.41	2.68	2.97	3.28	-2.762	0.006
Skewness	0.1848	0.3736	-0.0461	0.1243	0.3273	0.0428	0.2322	-0.1121	0.0362	0.1576	-1.684	0.092
Smoothness	0.0036	0.0011	0.0027	0.0037	0.0042	0.0034	0.0009	0.0027	0.0035	0.0040	-0.885	0.376
Root-Mean-Square Level	139.96	19.34	124.54	139.59	152.93	128.02	16.82	114.59	122.05	144.81	-2.694	0.007
Root-Sum-of-Squares Level	3100.03	410.35	2776.00	3072.68	3300.49	2734.86	505.64	2365.07	2710.30	3040.94	-3.503	0.000
1st Percentile	100.07	17.75	86.37	100.03	113.14	86.87	18.18	74.57	82.50	102.39	-2.954	0.003
3rd Percentile	107.12	18.43	91.25	107.11	118.85	94.36	17.31	83.00	89.61	109.75	-2.868	0.004
5th Percentile	111.22	18.41	95.75	110.25	123.00	98.46	17.00	87.00	94.00	112.78	-2.902	0.004
10th Percentile	117.40	18.82	101.50	116.50	129.75	104.50	16.87	93.15	99.50	117.90	-2.917	0.004
25th Percentile	127.46	19.05	110.50	125.00	141.25	114.79	16.85	103.00	109.00	129.75	-2.816	0.005
75th Percentile	149.80	20.06	134.25	149.00	164.25	138.61	17.23	124.25	132.50	156.00	-2.517	0.012
90th Percentile	160.69	20.93	144.18	159.50	175.40	149.12	17.69	133.25	142.00	167.00	-2.430	0.015
95th Percentile	167.97	21.56	150.25	167.63	182.20	155.69	18.38	138.81	150.00	173.99	-2.440	0.015
97th Percentile	173.29	22.13	155.77	172.00	185.94	159.91	19.14	142.25	153.50	179.78	-2.459	0.014
99th Percentile	182.80	24.94	165.05	180.21	194.61	167.99	19.67	148.95	161.18	185.75	-2.430	0.015

Table 3. Continued.

Globus pallidus	Control (40)					Delusional disorder (40)					Z	p
	Mean	Std. Deviation	Percentiles			Mean	Std. Deviation	Percentiles				
			25	50	75			25	50	75		
Entropy	3.82	0.29	3.67	3.84	4.01	3.81	0.42	3.61	3.90	4.05	-0.144	0.885
Uniformity	0.2176	0.0368	0.1934	0.2150	0.2420	0.2061	0.0431	0.1709	0.2033	0.2401	-1.376	0.169
Mean Local Entropy	2.76	0.20	2.66	2.81	2.90	2.78	0.32	2.62	2.81	2.94	-0.452	0.651
Mean Local Range	45.39	4.81	41.08	45.12	49.66	44.19	5.91	39.76	42.99	48.44	-1.116	0.264
Mean Local Standard Deviation	17.62	2.03	15.77	17.42	19.50	17.09	2.41	15.24	16.49	19.00	-1.241	0.214
Contrast	167.44	44.42	149.55	162.98	186.90	169.75	52.37	139.21	170.80	197.00	-0.010	0.992
Correlation	-0.0472	0.2603	-0.0625	-0.0157	0.0195	-0.0283	0.2097	-0.0561	-0.0257	-0.0035	-0.443	0.658
Energy	0.0021	0.0003	0.0019	0.0021	0.0022	0.0024	0.0008	0.0018	0.0023	0.0027	-1.771	0.077
Homogeneity	0.1681	0.0300	0.1563	0.1621	0.1693	0.1647	0.0293	0.1514	0.1629	0.1799	-0.183	0.855
<i>Higuchi Fractal Dimension</i>	<i>1.23</i>	<i>0.04</i>	<i>1.21</i>	<i>1.22</i>	<i>1.25</i>	<i>1.26</i>	<i>0.06</i>	<i>1.22</i>	<i>1.25</i>	<i>1.30</i>	<i>-2.877</i>	<i>0.004</i>
Katz Fractal Dimension	1.33	0.09	1.28	1.31	1.36	1.35	0.11	1.29	1.30	1.34	-0.010	0.992
Hausdorff Fractal Dimension	1.54	0.09	1.48	1.51	1.54	1.56	0.09	1.49	1.53	1.65	-1.328	0.184
<i>Box-Counting Fractal Dimension</i>	<i>1.54</i>	<i>0.10</i>	<i>1.48</i>	<i>1.51</i>	<i>1.53</i>	<i>1.58</i>	<i>0.10</i>	<i>1.49</i>	<i>1.56</i>	<i>1.68</i>	<i>-1.992</i>	<i>0.046</i>

Mann-Whitney U Test. NOTE: Indicators with $p < 0.05$ are bolded and italicized.

Results

Half of the 20 patients and half of the 20 control subjects were male and other half were female, and there was no significant difference between the groups (chi-square value = 0.000, $p = 1.000$). The mean age of the patient group was 39.35 ± 12.06 (1st, 2nd and 3rd quartiles: 36, 44, 51, respectively) years, while the mean age of the control group was 36.53 ± 9.51 (1st, 2nd and 3rd quartiles: 36, 38, 49, respectively) years and there was no significant difference between the groups according to age ($z = -0.783$, $p = 0.417$).

Although there were weak differences in a few parameters rarely, for all three nuclei, there was no significant difference between the right and left sides in almost all of the parameters. For this reason, the nuclei of both sides were taken as separate samples.

For all three nuclei, many texture analysis parameters differed from controls. The texture analysis parameters investigated for all three nuclei are presented in the tables (Tables 1,2,3) and Fig. 2. The average values of many parameters of histogram all three nuclei were decreased in DD patients ($p < 0.05$). Pixel Count of ROI value is observed to be significantly decreased in patients with DD in the putamen, indicating a dimensional decrease ($p = 0.004$). Additionally, a decrease in Fractal analysis values is observed in patients with DD ($p < 0.05$).

Discussion

With the rapid development and progress of neuroimaging methods, these methods have led to their frequent use to elucidate the etiopathogenesis of psychiatric diseases. As in many psychiatric disorders, it is known that the neurobiology of delusional disorder has not been fully elucidated and its etiopathogenesis has not been well explained [32–34].

Structural changes in delusional disorder appear to share features with, but to be less widespread than, those seen in schizophrenia, the disorder with which it appears to have the strongest links in terms of shared clinical features and outcome. Until recently, it was believed that the symptoms of delusional disorder were not compatible with any neuropathological findings. There is a lack of research regarding structural changes in delusional disorder. Previous studies, which are low in number, reported volume reductions in the medial frontal/anterior cingulate cortex, bilateral insula, orbitofrontal cortex and thalamus [14,15].

Theories basically postulate the basal ganglia in action selection and help decide which of several possible behaviors to perform at any given time, but empirical studies have shown that the primary function of the basal ganglia is to regulate the performance of voluntary movements. The “behavior change” effect in the basal ganglia is influenced by signals from many areas of the brain, including the prefrontal cortex, which plays an important role in executive functions. It has been hypothesized that the basal ganglia are responsible not only for motor movement selection, but also for the selection of further cognitive actions [35,36].

In this study, possible differences were investigated by focusing on the dorsal striatum and globus pallidum, and texture differences that human observers could not notice were determined.

Although the study was not on the volumetric changes of the nuclei, the area values obtained with the largest diameter ROI placement were not found to be significant since they did not differ except for the putamen, although they did not fully correspond to the volumetric equivalent. The small putamen area in delusional disorder patients may contradict this.

The present study had certain limitations. Since there were no previous studies that analyzed basal ganglia with texture analysis in patients with delusional disorder, we were not able to compare the study findings. Relatively small sample size of patients and controls was another major limitation of the study. Finally, since the study was conducted in a retrospective design, no evaluation could be made to measure the severity of the patients' disease.

Conclusion

The average “mean, median and maximum” values of all three nuclei were decreased in DD patients. The differences detected in the texture parameters for all three nuclei indicate that there is something different in the delusional disorder than in the normal controls. As this is a defining feature of this study, it is recommended to evaluate the causes and consequences of the differences with further studies based on imaging in different characters.

Availability of Data and Materials

The datasets used and/or analyzed during the current study are available from the corresponding author on reasonable request.

Author Contributions

MB designed the research study and SB performed the research and analyzed the data. Both authors contributed to editorial changes in the manuscript. Both authors read and approved the final manuscript. Both authors have participated sufficiently in the work and agreed to be accountable for all aspects of the work.

Ethics Approval and Consent to Participate

The entire study was conducted in accordance with the 2013 revised version of the 1964 Declaration of Helsinki. All procedures involving human subjects/patients were approved from Kanuni Sultan Süleyman Research and Training Hospital Local Ethics Committee (IRB: 07/07/2022 — 2022.07.176) and the patients were exempted from informed consent.

Acknowledgment

Not applicable.

Funding

This research received no external funding.

Conflict of Interest

The authors declare no conflict of interest.

References

- [1] Marneros A, Pillmann F, Wustmann T. Delusional disorders—are they simply paranoid schizophrenia? *Schizophrenia Bulletin*. 2012; 38: 561–568.
- [2] Opjordsmoen S. Delusional disorder as a partial psychosis. *Schizophrenia Bulletin*. 2014; 40: 244–247.
- [3] American Psychiatric Association, DSM-5 Task Force. Diagnostic and statistical manual of mental disorders: DSM-5. 5th edn. American Psychiatric Association: Washington, D.C. 2013.
- [4] Yamada N, Nakajima S, Noguchi T. Age at onset of delusional disorder is dependent on the delusional theme. *Acta Psychiatrica Scandinavica*. 1998; 97: 122–124.
- [5] Perälä J, Suvisaari J, Saarni SI, Kuoppasalmi K, Isometsä E, Pirkola S, *et al.* Lifetime prevalence of psychotic and bipolar I disorders in a general population. *Archives of General Psychiatry*. 2007; 64: 19–28.
- [6] Bhatia MS, Saha R, Doval N. Delusional Disorder in a Patient with Corpus Callosum Agenesis. *Journal of Clinical and Diagnostic Research*. 2016; 10: VD01–VD02.
- [7] Govind P, Subramanian K, Kumar S. Diagnostic and Therapeutic Implications of Organic Delusional Disorder due to Tuberculous Adrenitis. *Case Reports in Psychiatry*. 2022; 2022: 5056976.
- [8] Kendler KS. Demography of paranoid psychosis (delusional disorder): a review and comparison with schizophrenia and affective illness. *Archives of General Psychiatry*. 1982; 39: 890–902.
- [9] González-Rodríguez A, Seeman MV. Differences between delusional disorder and schizophrenia: A mini narrative review. *World Journal of Psychiatry*. 2022; 12: 683–692.
- [10] Pellegrini R, Muñoz Negro JE, Ottoni R, Cervilla JA, Tonna M. The Affective Core of Delusional Disorder. *Psychopathology*. 2022; 55: 244–250.
- [11] Morimoto K, Miyatake R, Nakamura M, Watanabe T, Hirao T, Suwaki H. Delusional disorder: molecular genetic evidence for dopamine psychosis. *Neuropsychopharmacology: Official Publication of the American College of Neuropsychopharmacology*. 2002; 26: 794–801.
- [12] Persico AM, Catalano M. Lack of association between dopamine transporter gene polymorphisms and delusional disorder. *American Journal of Medical Genetics*. 1998; 81: 163–165.
- [13] Debnath M, Das SK, Bera NK, Nayak CR, Chaudhuri TK. Genetic associations between delusional disorder and paranoid schizophrenia: A novel etiologic approach. *Canadian Journal of Psychiatry. Revue Canadienne De Psychiatrie*. 2006; 51: 342–349.
- [14] Vicens V, Radua J, Salvador R, Anguera-Camós M, Canales-Rodríguez EJ, Sarró S, *et al.* Structural and functional brain changes in delusional disorder. *The British Journal of Psychiatry: the Journal of Mental Science*. 2016; 208: 153–159.
- [15] Mermi O, Keles D, Kilic MC, Baykara S, Korkmaz S, Atmaca M. Orbitofrontal Cortex and Thalamus Volumes in Patients with Delusional Disorder. *Psychiatry and Behavioral Sciences*. 2021; 11: 72–79.
- [16] Alexander GE. Basal ganglia-thalamocortical circuits: their role in control of movements. *Journal of Clinical Neurophysiology: Official Publication of the American Electroencephalographic Society*. 1994; 11: 420–431.
- [17] Kasahara K, DaSalla CS, Honda M, Hanakawa T. Basal ganglia-cortical connectivity underlies self-regulation of brain oscillations in humans. *Communications Biology*. 2022; 5: 712.
- [18] Nusbaum F, Hannoun S, Kocevar G, Stamile C, Fournere P, Revol O, *et al.* Hemispheric Differences in White Matter Microstructure between Two Profiles of Children with High Intelligence Quotient vs. Controls: A Tract-Based Spatial Statistics Study. *Frontiers in Neuroscience*. 2017; 11: 173.
- [19] Lauterbach EC, Cummings JL, Duffy J, Coffey CE, Kaufer D, Lovell M, *et al.* Neuropsychiatric correlates and treatment of lenticulo-striatal diseases: a review of the literature and overview of research opportunities in Huntington's, Wilson's, and Fahr's diseases. A report of the ANPA Committee on Research. *American Neuropsychiatric Association. The Journal of Neuropsychiatry and Clinical Neurosciences*. 1998; 10: 249–266.
- [20] Lester J, Zúñiga C, Díaz S, Rugilo C, Micheli F. Diffuse intracranial calcinosis: Fahr disease. *Archives of Neurology*. 2006; 63: 1806–1807.
- [21] Schmidt U, Mursch K, Halatsch ME. Symmetrical intracerebral and

- intracerebellar calcification (“Fahr’s disease”). *Functional Neurology*. 2005; 20: 15.
- [22] Brandt GN, Bonelli RM. Structural neuroimaging of the basal ganglia in schizophrenic patients: a review. *Wiener Medizinische Wochenschrift (1946)*. 2008; 158: 84–90.
- [23] Castellano G, Bonilha L, Li LM, Cendes F. Texture analysis of medical images. *Clinical Radiology*. 2004; 59: 1061–1069.
- [24] Ganeshan B, Miles KA, Young RCD, Chatwin CR, Gurling HMD, Critchley HD. Three-dimensional textural analysis of brain images reveals distributed grey-matter abnormalities in schizophrenia. *European Radiology*. 2010; 20: 941–948.
- [25] Baykara S, Baykara M, Mermi O, Yildirim H, Atmaca M. Magnetic resonance imaging histogram analysis of corpus callosum in a functional neurological disorder. *Turkish Journal of Medical Sciences*. 2021; 51: 140–147.
- [26] Baykara M, Baykara S. Texture analysis of dorsal striatum in functional neurological (conversion) disorder. *Brain Imaging and Behavior*. 2022; 16: 596–607.
- [27] Yu H, Caldwell C, Mah K, Poon I, Balogh J, MacKenzie R, *et al.* Automated radiation targeting in head-and-neck cancer using region-based texture analysis of PET and CT images. *International Journal of Radiation Oncology, Biology, Physics*. 2009; 75: 618–625.
- [28] Ganeshan B, Panayiotou E, Burnand K, Dizdarevic S, Miles K. Tumour heterogeneity in non-small cell lung carcinoma assessed by CT texture analysis: a potential marker of survival. *European Radiology*. 2012; 22: 796–802.
- [29] Daniels DL, Houghton VM, Naidich TP. Cranial and spinal magnetic resonance imaging: an atlas and guide. Raven Press: New York. 1987.
- [30] Talairach J, Tournoux P. Co-planar stereotaxic atlas of the human brain. 3-Dimensional proportional system: an approach to cerebral imaging. George Thieme Verlag: New York. 1988.
- [31] Materka A. Texture analysis methodologies for magnetic resonance imaging. *Dialogues in Clinical Neuroscience*. 2004; 6: 243–250.
- [32] Harnett NG, van Rooij SJH, Ely TD, Lebois LAM, Murty VP, Jovanovic T, *et al.* Prognostic neuroimaging biomarkers of trauma-related psychopathology: resting-state fMRI shortly after trauma predicts future PTSD and depression symptoms in the AURORA study. *Neuropsychopharmacology: Official Publication of the American College of Neuropsychopharmacology*. 2021; 46: 1263–1271.
- [33] Kalmady SV, Paul AK, Narayanaswamy JC, Agrawal R, Shivakumar V, Greenshaw AJ, *et al.* Prediction of Obsessive-Compulsive Disorder: Importance of Neurobiology-Aided Feature Design and Cross-Diagnosis Transfer Learning. *Biological Psychiatry. Cognitive Neuroscience and Neuroimaging*. 2022; 7: 735–746.
- [34] Kraguljac NV, Lahti AC. Neuroimaging as a Window Into the Pathophysiological Mechanisms of Schizophrenia. *Frontiers in Psychiatry*. 2021; 12: 613764.
- [35] Stocco A, Lebiere C, Anderson JR. Conditional routing of information to the cortex: a model of the basal ganglia’s role in cognitive coordination. *Psychological Review*. 2010; 117: 541–574.
- [36] Chakravarthy VS, Joseph D, Bapi RS. What do the basal ganglia do? A modeling perspective. *Biological Cybernetics*. 2010; 103: 237–253.